FEL Oscillator Principles[1]

K.-J. Kim[1], *L. Ryan*[2] *and Z. Huang*[3]
[1]The University of Chicago, Illinois, USA
[2]Argonne National Lab, Illinois, USA
[3]Stanford University, California, USA

Abstract
In this lecture we discuss the principles of an FEL oscillator, in which a radiation pulse is trapped in an optical cavity but receives repeated amplification as the pulse meets an electron bunch as it come to the entrance of a low-gain FEL. We provide a qualitative picture of how the power and the longitudinal and transverse modes of the pulse develop.

Keywords
FEL oscillator; basic principles.

1. Introduction

The basic schematic of an FEL oscillator is illustrated in Fig. 1. Electron bunches from a (usually radiofrequency) accelerator pass through an undulator that is located inside a low-loss optical cavity. Starting from an empty cavity, in the first pass the electron beam emits spontaneous undulator radiation that is reflected back into the undulator by the cavity mirrors. In the second pass, the pulse of spontaneous emission meets and overlaps with a second electron bunch at the entrance of the undulator. The radiation and the e-beam interact in the undulator, after which the output field is composed of the spontaneous emission from both the first and second pass, along with an amplified signal due to FEL gain. This process repeats, so that the amplified radiation signal will eventually dominate the output if the gain is larger than the round-trip loss in the cavity.

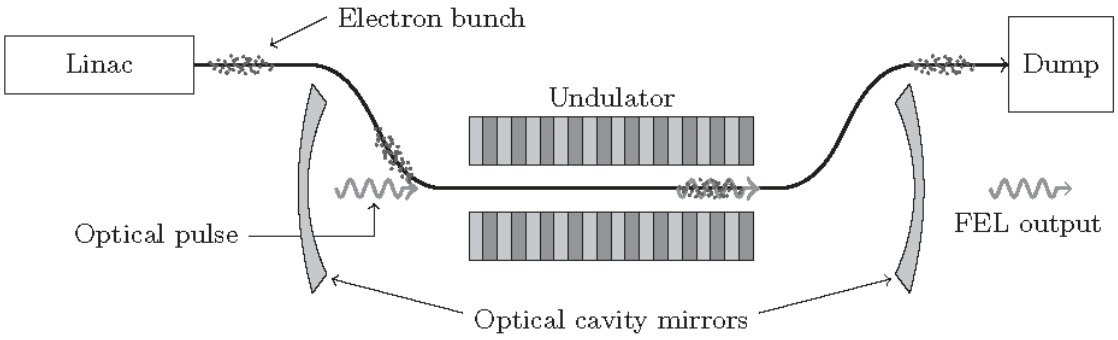

Fig. 1: Schematic of an FEL oscillator showing its basic operating principle

1 Power evolution and saturation

For a simple mathematical description of the power evolution in an oscillator, let P_n be the power of the optical pulse at the undulator exit after its nth pass, and P_s be the power of spontaneous emission. Then

[1]from Kwang-Je Kim, Zhirong Huang, Ryan Lindberg, Synchrotron Radiation and Free-Electron Lasers (2017), © Cambridge University Press 2017, reproduced with permission. This material cannot be reproduced, shared, altered, or exploited commercially in any way without the permission of Cambridge University Press, as it is copyrighted material and therefore not subject to the allowances permitted by a CC licence.

https://doi.org/10.23730/CYRSP-2018-001.493

$$P_1 = P_s\,,$$
$$P_n = R(1+G)P_{n-1} + P_s \quad \text{for } n \geq 2\,, \tag{1}$$

where G is the FEL gain and R is the reflectivity of the optical transport line. The net single pass power amplification is $R(1+G)$, and evidently the power increases if the single pass gain overcomes the losses such that

$$R(1+G) > 1\,. \tag{2}$$

This is the 'lasing' condition for an FEL oscillator. The power after the nth pass is governed by Eq. (1), whose solution is

$$P_n = \frac{[R(1+G)]^n - 1}{R(1+G) - 1} P_s\,. \tag{3}$$

Assuming that $R(1+G) > 1$, we see that the power increases exponentially with n after sufficiently many passes of amplification.

The exponential growth of the intracavity radiation power does not continue indefinitely. Rather, the optical power eventually becomes large enough to trap electrons in the ponderomotive potential and then rotate them to an absorptive phase where they extract energy from the field. This in turn reduces the gain from its small signal value, and the system reaches a steady state or 'saturates' when the gain decreases to the value G_{sat} given by

$$R(1+G_{\text{sat}}) = 1\,. \tag{4}$$

Furthermore, at saturation the power generated during one pass ΔP equals the total losses, so that if the power inside the cavity is P_{sat} we have $\Delta P = (1-R)P_{\text{sat}}$. It can be shown that $\Delta P \approx P_{\text{beam}}/2N_u$, which in turn implies that the intracavity optical power at saturation is

$$P_{\text{sat}} \approx \frac{1}{2N_u(1-R)} P_{\text{beam}}\,. \tag{5}$$

The optical elements in the cavity, and in particular the mirrors, must be able to withstand the power P_{sat} for the oscillator to operate stably.

At saturation the power decreases by an amount $(1-R)\Delta P$ during any complete round-trip cycle; this energy loss can be due to many different mechanisms, including radiation absorption in the mirror material, diffraction at the edges of the optical elements, and transmission out of the cavity for useful purposes. If one had an ideal optical line with no losses, the cavity transmission would equal $(1-R)$ so that the maximum power that can be coupled out of the oscillator is $(1-R)P_{\text{sat}} \approx P_{\text{beam}}/2N_u$.

Useful output radiation from an FEL oscillator requires it to operate for some time at saturation. Hence, an oscillator can be driven by a pulsed accelerator only if the number of bunches within each macro-pulse is more than that required to reach saturation. With a CW accelerator, on the other hand, the oscillator can be maintained at a steady state indefinitely. This is a desirable mode of operation, since the FEL then provides a stable source with a higher average photon flux.

2 Qualitative description of longitudinal mode development

There is much more physics at work in addition to the power evolution just described. One subtle but important phenomenon is lethargy (Ref. [1])—the fact that the trailing part of the optical pulse (the tail) is more strongly amplified than the front (the head). This is because the initially unmodulated electron beam must propagate some distance through the undulator to develop the density modulation that provides FEL gain, during which time the electron beam and its gain slips behind the field envelope. As a consequence, the FEL gain is maximized when the cavity length is slightly shorter than that given by

the exact synchronism condition (the synchronism condition is when the cavity length equals the distance between successive bunches).

The lethargy effect causes the round-trip time of the pulse envelope to be in general different from the round-trip time of the phase, since the latter is determined essentially by the cavity length. In other words, the phase fronts return to the undulator after a time approximately equal to the round-trip time in the cavity, while the peak of the pulse envelope arrives a time of order the slippage time $N_u\lambda_1/c$ after. To be more precise, any delay of the phase fronts is given by the imaginary part of the complex gain, which is small at peak gain.

Temporal coherence in an FEL oscillator is achieved by gain narrowing due to the FEL itself and also through spectral filtering provided by the cavity mirrors if their reflectivity is wavelength-dependent. The FEL-induced spectral gain narrowing occurs because the FEL gain is frequency dependent; alternatively, it can be understood as the slow increase in the coherence length from $N_u\lambda_1$ due to many passes through the undulator. Hence, when the mirror reflectivity is independent of wavelength, we expect that the FEL spectral bandwidth σ_ω decreases with pass number n as

$$\left(\frac{\sigma_\omega}{\omega_1}\right)_n \sim \frac{1}{N_u}\frac{1}{\sqrt{n}}. \tag{6}$$

For short electron bunches, gain narrowing stops when $(\sigma_\omega/\omega_1)_n$ becomes the transform limited bandwidth $\lambda_1/(4\pi\sigma_z)$ associated with the root mean square (RMS) length of the electron bunch σ_z. For longer electron bunches that have a current maximum in the centre, the non-uniform gain causes the optical pulse profile to also narrow in length/duration, with $(\Delta z)_n^{\mathrm{rms}} \sim \sigma_z/\sqrt{n}$. The spectral and temporal narrowing will stop when the pulse is determined by Fourier transform-limited, i.e., at the pass number $n \sim N_{\mathrm{FT}}$ determined by

$$\left(\frac{\sigma_\omega}{\omega_1}\right)_{N_{\mathrm{FT}}} (\Delta z)_{N_{\mathrm{FT}}}^{\mathrm{rms}} \sim \frac{\lambda_1}{4\pi}, \tag{7}$$

from which we determine that the steady state is reached after approximately $N_{\mathrm{FT}} \sim 4\pi\sigma_z/\lambda_1 N_u$ passes, and that the limiting bandwidth is, as seen in Ref. [2]

$$\frac{\sigma_\omega}{\omega_1} \sim \sqrt{\frac{\lambda_1}{4\pi N_u \sigma_z}}. \tag{8}$$

This limiting mode is known as the dominant supermode, see Ref. [3].

In what follows we will show how the longitudinal supermodes arise from the dynamic interplay between amplification, gain narrowing, FEL lethargy, and spectral filtering from the mirrors. Hence, we will further extend the physics above to include the possibility that the spectral narrowing comes about not only through slippage, but also because the mirrors have a limited bandpass.

3 Longitudinal supermodes of the FEL oscillator

In this section we use the simple low-gain model developed by Elleaume [4] to more fully investigate the supermode longitudinal dynamics. This model divides the evolution during a single round trip into its various components: gain that depends on the current and the propagation/slippage in the undulator, reflection by the mirrors, and propagation in the cavity. Assuming that all of these effects result in small perturbations to the radiation (as is true in the low-gain regime), then we can approximate each as acting individually and in succession on the electric field $E(t)$. We discuss these longitudinal effects in turn, and then combine them into a single equation describing the linear dynamics of a low-gain oscillator.

We assume that the FEL gain transforms the field via the amplification operator $E \to E + \mathcal{G}[E]$. To develop a simple model for, we recall that FEL gain depends linearly on the current and that the field interacts with the electron beam within one slippage length $N_u\lambda_1$. In terms of the light-cone coordinate $\tau \equiv z - ct$, this means that the amplification of $E(\tau)$ depends on the interaction between the current and field amplitude for points τ' satisfying $\tau \le \tau' \le \tau + N_u\lambda_1$ (see, for example, [5]). We will use a very simple description of this process in which we model the gain operation $\mathcal{G}[E]$ as increasing the field by an amount depending on the e-beam current and *E*-field amplitude at the point one-half the slippage distance $N_u\lambda_1/2$ ahead. Hence, we approximate the amplitude gain from an electron beam with RMS length σ_z as acting via

$$\begin{aligned} E(\tau) \to E(\tau) + \mathcal{G}[E] &\approx E(\tau) + \frac{G}{2}\mathrm{e}^{-(\tau+N_u\lambda_1/2)^2/2\sigma_z^2} E\left(\tau + \frac{1}{2}N_u\lambda_1\right) \\ &\approx \left[1 + \frac{G}{2}\left(1 - \frac{t^2}{2\sigma_z^2}\right)\right] E(\tau) \\ &\quad + \frac{G}{4}N_u\lambda_1 \frac{\partial E}{\partial \tau} + \frac{G}{16}(N_u\lambda_1)^2 \frac{\partial^2 E}{\partial \tau^2}\,, \end{aligned} \tag{9}$$

where for simplicity we assume that $\sigma_z \gg N_u\lambda_1$ and that the amplitude gain $G/2$ is real[2].

After the FEL interaction, the mirror reduces the field amplitude by the multiplicative factor $\sqrt{R} \equiv \sqrt{1-\alpha} \approx 1 - \alpha/2$, where α is the (assumed real) power loss. In addition, we include the possibility that the reflectivity depends on frequency by modelling it as a Gaussian filter in ω with RMS power bandwidth σ_{refl}. Since we model the mirror filtering as acting on the slowly-varying field envelope, it is centred near $\omega = 0$ and results in the transformation

$$\begin{aligned} E(\tau) \to \int \mathrm{d}\omega\, \mathrm{e}^{-\mathrm{i}\omega\tau/c} R(\omega) E(\omega) &\approx (1 - \alpha/2) \int \mathrm{d}\omega\, \mathrm{e}^{-\mathrm{i}\omega\tau/c} \mathrm{e}^{-\omega^2/4\sigma_{\mathrm{refl}}^2} E(\omega) \\ &\approx \left(1 - \frac{\alpha}{2}\right) \int \mathrm{d}\omega\, \mathrm{e}^{-\mathrm{i}\omega\tau/c} \left[1 - \frac{\omega^2}{4\sigma_{\mathrm{refl}}^2}\right] E(\omega) \\ &= \left(1 - \frac{\alpha}{2}\right) E(\tau) + \frac{c^2}{4\sigma_{\mathrm{refl}}^2} \frac{\partial^2}{\partial \tau^2} E(\tau). \end{aligned} \tag{10}$$

Finally, we include the possibility that after one round trip through the cavity the arrival time of the radiation pulse and the next electron bunch may differ by an amount ℓ/c; this timing difference, called *detuning* in the FEL community, could be due to adjustments to the cavity length or timing jitter of the electrons; we model it by

$$E(\tau) \to E(\tau + \ell) \approx E(\tau) + \ell \frac{\partial}{\partial \tau} E(\tau)\,. \tag{11}$$

A full pass through the oscillator is composed of the transformation Eqs. (9)–(11) due to the gain including slippage, the mirror, and the cavity length detuning. Every transformation is written as a sum of the initial field $E(\tau)$ and a perturbation. If each of these perturbing effects is small, then the field at pass $(n+1)$ can be written a sum of the various perturbations acting on the field E_n as follows:

$$\begin{aligned} E_{n+1}(\tau) &\approx E_n(\tau) + \frac{G - \alpha}{2} E_n(\tau) - \frac{G\tau^2}{4\sigma_z^2} E_n(\tau) \\ &\quad + \left(\ell + \frac{GN_u\lambda_1}{4}\right) \frac{\partial E_n}{\partial \tau} + \left[\frac{c^2}{4\sigma_{\mathrm{refl}}^2} + \frac{G(N_u\lambda_1)^2}{16}\right] \frac{\partial^2 E_n}{\partial \tau^2}\,. \end{aligned} \tag{12}$$

[2] The generalization to complex *G* and $\sqrt{R}$ is straightforward but messy. For example, the change in power is $|1 + G/2|^2 \approx 1 + (G + G^*)/2$ if *G* is complex.

Moving E_n to the left-hand side and setting $E_{n+1} - E_n \approx \partial E_n/\partial n$ leads to a linear partial differential equation for the field $E_n(\tau)$. This PDE can be solved by the separation of variables technique, which leads to exponential dependence on n, while the temporal variation is described by Hermite–Gauss functions. We index these linear modes by p and find that the general solution can be written as a sum over the 'supermodes'

$$E_n^p(\tau) = \exp\left[\left(\frac{G-\alpha}{2}\right)n - \left(\frac{2D^2\sigma_{\text{filter}}^2}{c^2} + \frac{c(1+2p)\sqrt{G}}{2\sigma_z\sigma_{\text{filter}}}\right)n\right] \times \mathrm{e}^{-2\sigma_{\text{filter}}^2 D\tau/c^2}\exp\left[-\frac{\sqrt{G}c\sigma_{\text{filter}}}{\sigma_z}\tau\right]H_p\left(G^{1/4}\sqrt{\frac{c\sigma_{\text{filter}}}{\sigma_z}}\tau\right), \tag{13}$$

where we have defined the net detuning length $D \equiv \ell + GN_u\lambda_1/4$ and the effective filtering bandwidth σ_{filter} via

$$\frac{1}{\sigma_{\text{filter}}^2} \equiv \frac{1}{\sigma_{\text{refl}}^2} + \frac{GN_u^2\lambda_1^2}{16}. \tag{14}$$

The first line in Eq. (13) indicates that the exponential power growth is reduced from its nominal value $G-\alpha$ (gain minus loss) if the total detuning length $D \neq 0$; this condition shows one effect of lethargy since maximum gain is achieved when the cavity length is reduced slightly from its nominal synchronous length (i.e., $D = 0$ implies that $\ell < 0$). Significant FEL gain requires the total detuning to be within the effective oscillator bandwidth such that $D\sigma_{\text{filter}} \ll 1$. Additionally, setting $D = 0$ shows that the gain approaches the infinite beam limit only if the electron beam is also significantly longer than the inverse bandwidth $1/\sigma_{\text{filter}}$. For shorter electron bunches, only the fraction of current whose spectral content lies within the effective bandpass set by either the mirror σ_{refl} or the slippage $4/(N_u\lambda_1\sqrt{G})$ contributes to the gain.

The RMS width of the pth mode is proportional to the geometric mean of the e-beam size and $1/\sigma_{\text{filter}}$, with temporal width $\sim\sqrt{(1+2p)\sigma_z/c\sigma_{\text{filter}}}$. When the electron bunch is long there are many longitudinal modes with comparable growth rates, and the oscillator output is comprised of a superposition of supermodes whose total bandwidth $\sim 1/N_u$ and temporal duration $\sim\sigma_z$. As the evolution proceeds through many passes, however, the lowest-order ($p = 0$) Gaussian mode with largest gain will eventually become dominant. If the mirror is essentially wavelength independent, $\sigma_{\text{refl}} \gg 1/N_u\lambda_1$, our discussion in the beginning of this chapter applies and the output bandwidth will approach the limiting value Eq. (8), albeit slowly.

On the other hand, we will see that the crystal mirrors that enable FEL oscillators in the X-ray spectral region have $\sigma_{\text{refl}} \ll 1/N_u\lambda_1$ (typically $N_u \lesssim 3\times10^3$ while $\sigma_{\text{refl}}/\omega_1 \sim 10^{-5}$ to 10^{-7}). In this case, $\sigma_{\text{filter}} \to \sigma_{\text{refl}}$ which simplifies some of the preceding discussion. For example, the lowest-order (Gaussian) supermode simplifies to

$$E_n^0(\tau) = \exp\left[\frac{1}{2}\left(G - R - \frac{4\ell^2\sigma_{\text{refl}}^2}{c^2} - \frac{c\sqrt{G}}{\sigma_z\sigma_{\text{refl}}}\right)n\right]\mathrm{e}^{-2\sigma_{\text{refl}}^2 l\tau/c^2}\mathrm{e}^{-\tau^2/2\sigma_0^2}, \tag{15}$$

where the mean square temporal width $\sigma_0^2 \equiv \sigma_z/\left(\sqrt{G}c\sigma_{\text{refl}}\right)$. Hence, in this case the gain is reduced from its nominal value if either the cavity length shift ℓ or the electron beam width σ_z is smaller than the inverse bandwidth of the mirror c/σ_{refl}. The steady state temporal width is given by $\sigma_0 \propto \sqrt{\sigma_z/c\sigma_{\text{refl}}}$ with final bandwidth $\propto\sqrt{c\sigma_{\text{refl}}/\sigma_z}$, and it now requires $N_{\text{FT}} \sim 2\sigma_{\text{refl}}\sigma_z/c \ll 4\pi\sigma_z/(\lambda_1 N_u)$ passes to reach this steady state.

In addition to modifying the supermode behaviour, the additional spectral filtering provided by the mirrors also completely suppresses the sideband/synchrotron instability, eliminating the unstable

and chaotic 'spiking mode' of operation observed at lower wavelengths, example [6, 7]. This is because the sideband instability amplifies frequency content near that associated with the synchrotron period, i.e., with frequencies at = $\omega_1 \pm \omega_s$, where

$$\omega_s \sim \frac{\lambda_u}{\lambda_1} c k_s = \frac{\lambda_u}{\lambda_1} \frac{c}{L_u} \sqrt{\epsilon} = \frac{c}{N_u \lambda_1} \sqrt{\epsilon} \,, \tag{16}$$

where ϵ is the normalized field strength. At saturation $\epsilon \sim 1$, so that the characteristic frequency of the sideband/'spiking' mode is

$$\omega_s \sim \frac{c}{N_u \lambda_1} \gg \sigma_{\text{refl}} \,, \tag{17}$$

and the narrow bandwidth of the XFELO crystal mirrors effectively filters out the sideband instability.

4 Transverse physics of the optical cavity

When the gain is small, the transverse mode is typically well described by the vacuum resonator modes of the cavity. We will briefly describe some of the transverse cavity physics in the limit of Gaussian optics, which assumes that angles from the optical axis are small (paraxial) and that optical elements can be treated as producing linear transformations to the field. The linear transformations propagate the radiation brightness/Wigner function along rays, which implies that we can analyse the cavity modes using the same matrix formulation for particle beams. Under these limiting circumstances, the transformations act on the (pseudo)-distribution of rays in the position–angle phase space $(\boldsymbol{x}, \boldsymbol{\phi})$, and the wave behaviour can be described by referencing only the propagation of rays[3].

In the laser community the matrix approach is referred to as the ABCD-matrix method, see Ref. [8], and typically these matrix elements are used to derive the stable Rayleigh range and wavefront curvature for Hermite–Gaussian cavity modes. The lowest-order mode is analogous to a Gaussian particle beam with emittance $\lambda/4\pi$, while its Rayleigh length at the waist $Z_R = \sigma_r^2/(\lambda/4\pi) = (\lambda/4\pi)\sigma_r'^2$, is equivalent to the Courant–Snyder beta function from particle optics.

In order to understand the transverse X-ray profile, we first consider the simple two-mirror resonator. We model this optical cavity as containing one ideal mirror of focal length f, such that the round-trip distance in the cavity is L_c. We restrict our discussion to the two-dimensional phase space (x, ϕ), and using the fact that the matrices associated with a drift length ℓ and a focusing mirror are, respectively,

$$\mathsf{L}(\ell) = \begin{bmatrix} 1 & \ell \\ 0 & 1 \end{bmatrix}, \qquad \mathsf{F}(f) = \begin{bmatrix} 1 & 0 \\ -1/f & 1 \end{bmatrix}. \tag{18}$$

Stable resonator modes exist when the RMS size, divergence, and correlation are periodic over one round trip through the cavity. These mode sizes can be determined from the matrix map that starts and ends in the middle of the undulator; for the two-mirror resonator this is given by $\mathsf{M}_{2\text{res}} = \mathsf{L}(L_c/2)\mathsf{F}(f)\mathsf{L}(L_c/2)$. The matrix $\mathsf{M}_{2\text{res}}$ maps (x, ϕ) from and back to the centre of the cavity such that

$$\begin{bmatrix} x \\ \phi \end{bmatrix}_{\text{out}} = \mathsf{M}_{1\text{res}} \begin{bmatrix} x \\ \phi \end{bmatrix}_{\text{in}} , \tag{19}$$

[3] Non-ideal elements, apertures, and nonlinear transformations introduce interference effects that may not be well described by the methods presented here.

while the second-order moment matrix Σ_{out} at the output plane is related to the initial Σ_{in} via

$$\Sigma_{\mathrm{out}} \equiv \begin{bmatrix} \langle x^2 \rangle & \langle x\phi \rangle \\ \langle \phi x \rangle & \langle \Phi^2 \rangle \end{bmatrix}_{\mathrm{out}} = \mathsf{M}_{2\mathrm{res}} \begin{bmatrix} \langle x^2 \rangle & \langle x\phi \rangle \\ \langle \phi x \rangle & \langle \phi^2 \rangle \end{bmatrix}_{\mathrm{in}} \mathsf{M}_{2\mathrm{res}}^{T}$$
$$= \mathsf{M}_{2\mathrm{res}} \Sigma_{\mathrm{in}} \mathsf{M}_{2\mathrm{res}}^{T} . \tag{20}$$

Equating Σ_{out} and Σ_{in} implies that at the cavity middle the correlation vanishes (the radiation has a waist), and that the cavity round trip length L_c and mirror focal length f are related to the trapped mode Rayleigh length through the following relation:

$$f = \frac{L_c}{4} + \frac{1}{L_c} \frac{\langle x^2 \rangle_{\mathrm{in}}}{\langle \phi \rangle_{\mathrm{in}}} = \frac{L_c}{4} + \frac{z_R^2}{L_c} . \tag{21}$$

Note that stable operation requires $f > L_c/4$, which in terms of the mirror's radius of curvature is $2f = r > L_c/2$. This inequality can be violated if there is sufficient FEL amplification, but for low-gain devices it provides a good starting point for optical cavity design.

References

[1] H. Al-Abawi, F.A. Hoff, G.T. Moore and M.O. Scully, *Opt. Comm.* **30** (1979) 235. https://doi.org/10.1016/0030-4018(79)90085-3

[2] K.-J. Kim, *Phys. Rev. Lett.* **66** (1991) 2746. https://doi.org/10.1103/physrevlett.66.2746

[3] G. Dattoli, G. Marino, A. Renieri and F. Romanelli, *IEEE J. Quantum Electron*. **17** (1981) 1371. https://doi.org/10.1109/jqe.1981.1071268

[4] P. Elleaume, *IEEE J. Quantum Electron.* **21** (1985) 1012. https://doi.org/10.1109/jqe.1985.1072746

[5] T.M. Antonsen and B. Levush, *Phys. Fluids B: Plasma Phys.* **1** (1989) 1097. https://doi.org/10.1063/1.858980

[6] R.W. Warren, J.E. Sollid, D.W. Feldman, W.E. Stein, W.J. Johnson, A.H. Lumpkin and J.C. Goldstein, *Nucl. Instrum. Methods Phys. Res., Sect. A* **285** (1989) 1. https://doi.org/10.1016/0168-9002(89)90417-8

[7] R. Hajima, N. Nishimori, R. Nagai and E.J. Minehara, *Nucl. Instrum. Methods Phys. Res., Sect. A* **475** (2001) 270. https://doi.org/10.1016/s0168-9002(01)01621-7

[8] A.E. Siegman, *Lasers* (University Science Book, Sausalito, CA 1986).